RSC Advances

COMMUNICATION

View Article Online
View Journal | View Issue

Cite this: *RSC Adv.*, 2016, **6**, 103328

Iron–nickel hexacyanoferrate bilayer as an advanced electrocatalyst for H_2O_2 reduction†

Elena V. Karpova, Elena E. Karyakina and Arkady A. Karyakin*

Received 28th September 2016
Accepted 16th October 2016

DOI: 10.1039/c6ra24128j

www.rsc.org/advances

An advanced electrocatalyst for H_2O_2 reduction was synthesized *via* the deposition of an iron- and nickel hexacyanoferrate bilayer and displayed a similar electrocatalytic activity ($\approx$0.01 cm s^{-1}) and an almost 100-fold improved operational stability compared to Prussian Blue. The electrocatalyst was highly reproducible, with a deviation in both the operational stability and catalytic activity among different modified electrodes of <10%.

Hydrogen peroxide (H_2O_2) fuel cells proposed almost 50 years ago[1] comprise an important part of modern energetics. In particular, for air-deficient conditions (such as for space power systems[2]) hydrogen peroxide fuel cells are proposed involving the oxidation of methanol,[1,3] hydrazine,[4] borohydride,[5,6] aluminium,[7,8] or zinc[9] at the anode.

Electrocatalysis is the key process in fuel cells and allows achievement of a high energy output. Depending on the electrocatalysts used, hydrogen peroxide can even play a dual role in fuel cells, serving as both an oxidant and a fuel.[10] The most important reaction, however, is H_2O_2 reduction. In this regard, several electrocatalysts have already been reported, from peroxidase[11] to porphyrin,[12] and, more recently, Prussian Blue.[6,13,14]

Prussian Blue as a selective electrocatalyst for hydrogen peroxide reduction was discovered by our group more than 20 years ago.[15] Compared to platinum, Prussian Blue-modified electrodes are: (i) three orders of magnitude more active in H_2O_2 reduction and oxidation in terms of the electrochemical rate constant,[16] and (ii) three orders of magnitude more selective for hydrogen peroxide reduction in the presence of oxygen.[17] The main applications of Prussian Blue so far have been in the elaboration of sensors and biosensors with advantageous analytical performances.[17–19] Prussian Blue-based nanoelectrode arrays[20] have helped such electrochemical sensors achieve record performance characteristics.[21]

The main (perhaps, the only) disadvantage of Prussian Blue is its poor operational stability, whereby the hydroxyl ion (OH^-), which is a product of H_2O_2 reduction,[22] is able to solubilize ferric hexacyanoferrate. The use of non-iron hexacyanoferrates for hydrogen peroxide reduction have consequently now been reported to overcome this issue; however, their efficacy is several orders of magnitude lower than Prussian Blue.[17,23–26] Moreover, as we recently found, non-iron transition metal hexacyanoferrates are inactive in H_2O_2 reduction: their apparent catalytic activity otherwise is only due to the presence of Prussian Blue as defects in their structure.[27]

Hence, the best methods to synthesize advanced electrocatalysts for H_2O_2 reduction with improved operational stability should be based on the stabilization of Prussian Blue. Different strategies have been already used for this aim, such as covering with organic polymers[28,29] or multilayers of non-iron hexacyanoferrates isostructural to Prussian Blue[30,31] or entrapment in sol–gel[32–34] or conductive polymer matrices.[35,36] However, despite the stabilization effects achieved so far, the resulting electrocatalytic materials are characterized by a decreased catalytic activity and, in particular, poor reproducibility.

In this work, we report an advanced electrocatalyst for hydrogen peroxide reduction. Compared to Prussian Blue, which as previously stated is known to be a superior electrocatalyst in this reaction, the resulting material displays similar catalytic activity (*e.g.* an electrochemical rate constant of $\approx$0.01 cm s^{-1}) with a two orders of magnitude improved operational stability.

Since the simultaneous deposition of iron- and nickel hexacyanoferrates does not result in significant improvements in operational stability of the final hybrid material,[30] we investigated the possibility for its deposition as a bilayer. Obviously, the labile electrocatalyst (*e.g.* Prussian Blue) has to be deposited initially and then covered with a stabilizing layer (NiHCF). Synthesis was carried out in cyclic voltammetric conditions (see the ESI† for details). Whereas the separate deposition of

Chemistry Faculty of M.V. Lomonosov Moscow State University, Moscow, 119991, Russia. E-mail: karyakin@analyt.chem.msu.ru

† Electronic supplementary information (ESI) available. See DOI: 10.1039/c6ra24128j

transition metal hexacyanoferrates is well known, their sequential deposition has not been characterized yet. Fig. 1 displays the deposition of nickel hexacyanoferrate over Prussian Blue-modified electrodes. Whereas the cathodic set of peaks remains unchanged, a continuous growth of electroactivity above 0.6 V can be observed. The anodic set of peaks are not observed for Prussian Blue, hence they can be attributed to nickel hexacyanoferrate. The inset in Fig. 1 displays a typical cyclic voltammogram of the PB–NiHCF bilayer. Sets of peaks of the PB and NiHCF electroactivities are well separated, which allows us to calculate the amount of each hexacyanoferrate.

Both high operational stability and high electrocatalytic activity of the resulting material are desirable. The operational stability of the modified electrode can be characterized by the time the current is retained at >95% of its initial value ($t_{95\%}$) under hard conditions of a continuous flow of 1 mM H_2O_2 in a wall-jet cell. In a wall-jet cell, a jet of solution is issued from a circular nozzle to impinge normally on a disc electrode. Hence, the reasonable optimization parameter is the sensitivity (S) multiplied by $t_{95\%}$. Since the current response of Prussian Blue-modified electrodes towards hydrogen peroxide addition is linear over a wide concentration range, the sensitivity can be determined as the current under a continuous flow of 1 mM H_2O_2 divided by the concentration (1 mM). Chronoamperometry was carried out at a potential of 0.0 V (Ag|AgCl) when the current from hydrogen peroxide reduction at the Prussian Blue-modified electrodes reaches its limiting plateau region.

Fig. 2 displays the optimization parameters as a function of both iron- and nickel hexacyanoferrate surface coverage. These were calculated integrating the current peaks in the cyclic voltammograms assuming a transfer of 4 electrons per unit cell. As seen, the 3D plot is a sharp hill with the optimum amount of Prussian Blue being 1.2 ± 0.1 nmol cm^{-2} covered with 2.5 ± 0.6 nmol cm^{-2} nickel hexacyanoferrate. Except for the chosen optimization parameter, at this particular surface coverage, the highest operational stability of the resulting electrocatalyst is achieved. We note, however, that electrochemical deposition on other surfaces may result in different optimum amounts.

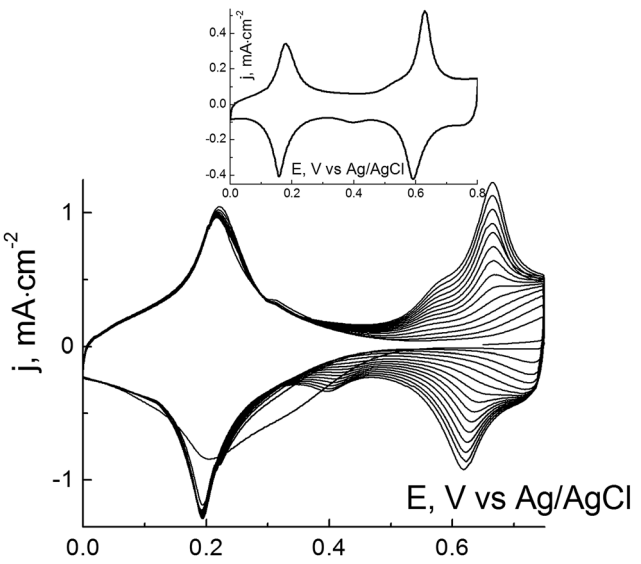

Fig. 1 Deposition of NiHCF over a Prussian Blue-modified electrode; 0.1 M HCl and 0.5 M KCl, sweep rate of 0.1 V s^{-1}. Inset: cyclic voltammograms of the PB–NiHCF bilayer; 0.1 M HCl and 0.1 M KCl, sweep rate of 0.04 V s^{-1}.

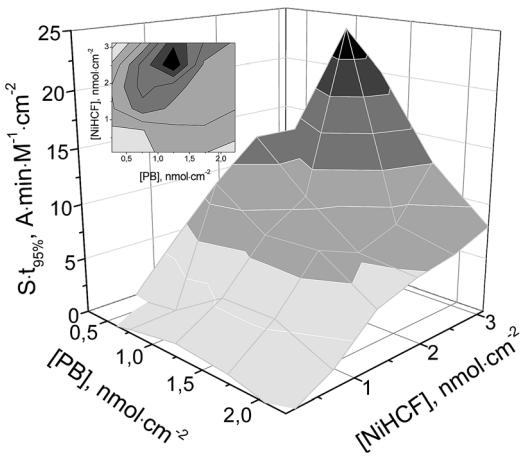

Fig. 2 Sensitivity multiplied by $t_{95\%}$ as a function of surface coverage for iron- and nickel hexacyanoferrates in a continuous flow (0.8 ml min^{-1}) in a wall-jet cell; 0.05 M phosphate buffer pH 6.0 with 0.1 M KCl.

As known, at a surface coverage of >1 nmol cm^{-2} Prussian Blue covers the entire electrode surface completely. The electrocatalyst is of a polycrystalline nature with crystalline dimensions less than 100 nm.[21] The layer thickness, determined by AFM, was found to be about 60–80 nm.[21] The Prussian Blue cyclic voltammogram remains unchanged during the deposition of nickel hexacyanoferrate, hence it does not disturb the PB layer. NiHCF is also expected to be deposited at its regular morphology.

As mentioned, the highest values of both catalytic activity and operational stability are achieved with a similar amount of Prussian Blue (1.2 ± 0.1 nmol cm^{-2}). The material synthesized in the course of applying a lower (*e.g.* 1.6 nmol cm^{-2}) amount of stabilization layer displays a 30–40% higher response towards hydrogen peroxide (Fig. 1S, ESI†). For further study, we chose the hybrid iron–nickel hexacyanoferrate material as it displayed both the highest operational stability and the highest multiplication of $t_{95\%}$ by sensitivity (Fig. 2).

As mentioned, the operational stability was investigated under hard conditions of continuous flow of 1 mM H_2O_2 in a wall-jet flow-through cell. Under such conditions, Prussian Blue-modified electrodes, independently of the hexacyanoferrate amount deposited, lost 50% of their catalytic current within less than 20 min (Fig. 2S, ESI†). On the contrary, the synthesized hybrid material in similar conditions did not display any current decay within the first 50 min. Considering the aforementioned parameter characterizing the operational stability (*i.e.* $t_{95\%}$), for conventional Prussian Blue under such hard conditions it is equal to only 1–1.5 minutes. For the PB–NiHCF bilayer in similar conditions, $t_{95\%}$ was at more than 80 min (Fig. 2S, ESI†). This illustrates the tremendous, indeed almost two orders of magnitude, improvement in operational stability of the synthesized electrocatalyst.

The proposed synthetic procedure provides high reproducibility in terms of both catalytic activity and operational stability of the resulting material. Among six different modified electrodes synthesized with the optimum $St_{95\%}$ (Fig. 1), the standard deviation for both sensitivity (S) and operational stability ($t_{95\%}$) was less than 10%. The achieved high reproducibility ensures the electrocatalyst is of technological value.

The hybrid Fe–Ni hexacyanoferrate was also characterized by high electrochemical activity. The current response of the electrode modified with a thin (0.85 nmol cm^{-2}) Prussian Blue film was the same as in the case of Fe–Ni hexacyanoferrate (Fig. 2S, ESI†). This pricks an interest to investigate the catalytic properties of the synthesized hybrid material.

The electrochemical rate constant of the synthesized electrocatalyst was determined in forced hydrodynamic conditions by varying the flow rate in a wall-jet cell, as described in ref. 16. Accordingly, the recorded reciprocal current was plotted against the volume flow rate in the power of −0.75 (Fig. 3S, ESI†). The slopes and intercepts of the obtained linear dependencies represent the diffusion (j_D) and the kinetic (j_{kin}) terms of the current, respectively.[16] Both terms as functions of hydrogen peroxide concentration are displayed in Fig. 3. As seen, the dependencies are linear and intersect the origin as expected.

From the dependence of the diffusion term on the hydrogen peroxide concentration, the diffusion coefficient (D) for H_2O_2 can be evaluated. By recalculating the data displayed in Fig. 3 according to ref. 16 the diffusion coefficient of $D_{H_2O_2} = 8.8 \pm 0.2 \times 10^{-6}$ cm^2 s^{-1} is obtained. This value is in an excellent agreement with the literature data.[37] Such an agreement is an independent validation of the forced hydrodynamic method used.

The electrochemical rate constant is calculated from the dependence of the kinetic current term on the hydrogen peroxide concentration. The obtained value for the electrochemical rate constant is $k_{el} = 9.7 \pm 0.2 \times 10^{-3}$ cm s^{-1}. A similar electrochemical rate constant was found for thin Prussian Blue films.[16] Hence, the catalytic activity of the Fe–Ni hexacyanoferrate bilayer is similar to that of conventional Prussian Blue, indicating it is a superior electrocatalyst for hydrogen peroxide reduction.

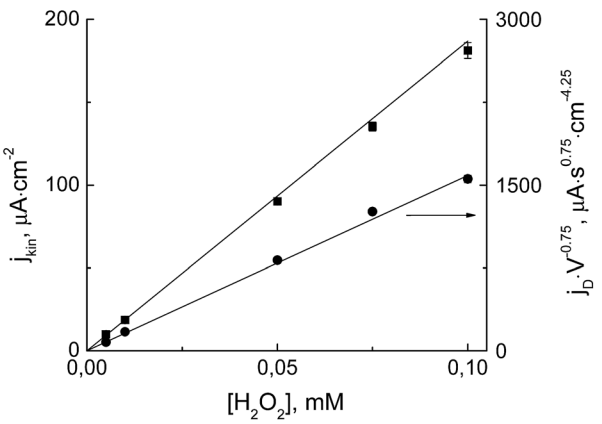

Fig. 3 Kinetics of H_2O_2 reduction onto Fe–Ni hexacyanoferrate: the diffusion (●) and kinetic (■) terms of the current as functions of hydrogen peroxide concentration; 0.05 M phosphate buffer pH 6.0 with 0.1 M KCl.

We conclude that an advanced electrocatalyst for hydrogen peroxide reduction was synthesized. This uses Prussian Blue, which is known to be 1000 times more active and selective than platinum in this reaction and has already found applications in H_2O_2 fuel cells; however, it suffers from poor operational stability. On the contrary, the reported PB–nickel hexacyanoferrate (NiHCF) bilayer is characterized by a tremendously improved operational stability, retaining its catalytic activity at a similar level to PB's high level (with an electrochemical constant of 0.01 cm s^{-1}). The PB–NiHCF bilayer is highly reproducible: deviations in both operational stability and catalytic activity of the final hybrid material are <10%, thus confirming its technological value. The superior characteristics of the electrocatalyst could open new horizons for hydrogen peroxide fuel cells. Alternatively, the electrocatalyst for H_2O_2 reduction could find applications in the elaboration of novel sensors and biosensors.

Acknowledgements

Financial support through Russian Science Foundation grant # 16-13-00010 is greatly acknowledged.

References

1 C. Iwakura, H. Tamura and T. Ishino, *J. Electrochem. Soc. Jpn.*, 1968, **36**, 107.
2 N. Luo, G. H. Miley, R. Gimlin, R. Burton, J. Rusek and F. Holcomb, *J. Propul. Power*, 2008, **24**, 583–589.
3 D. N. Prater and J. J. Rusek, *Appl. Energy*, 2003, **74**, 135–140.
4 H. Ichino, M. Yamashit and M. Kubokawa, *Nippon Kagaku Kaishi*, 1974, 669–672.
5 G. H. Miley, N. Luo, J. Mather, R. Burton, G. Hawkins, L. Gu, E. Byrd, R. Gimlin, P. J. Shrestha, G. Benavides, J. Laystrom and D. Carroll, *J. Power Sources*, 2007, **165**, 509–516.
6 G. Selvarani, S. K. Prashant, A. K. Sahu, P. Sridhar, S. Pitchumani and A. K. Shukla, *J. Power Sources*, 2008, **178**, 86–91.
7 R. R. Bessette, J. M. Cichon, D. W. Dischert and E. G. Dow, *J. Power Sources*, 1999, **80**, 248–253.
8 D. J. Brodrecht and J. J. Rusek, *Appl. Energy*, 2003, **74**, 113–124.
9 L. An, T. S. Zhao, X. L. Zhou, X. H. Yan and C. Y. Jung, *J. Power Sources*, 2015, **275**, 831–834.
10 S.-i. Yamazaki, Z. Siroma, H. Senoh, T. Loroi, N. Fujiwara and K. Yasuda, *J. Power Sources*, 2008, **178**, 20–25.
11 A. Pizzariello, M. Stred'ansky and S. Miertus, *Bioelectrochemistry*, 2002, **56**, 99–105.
12 R. K. Raman and A. K. Shukla, *J. Appl. Electrochem.*, 2005, **35**, 1157–1161.
13 S. A. M. Shaegh, N. Nam-Trung, S. M. M. Ehteshami and S. H. Chan, *Energy Environ. Sci.*, 2012, **5**, 8225–8228.
14 X. H. Yan, T. S. Zhao, L. An, G. Zhao and L. Shi, *Int. J. Hydrogen Energy*, 2016, **41**, 5135–5140.

15 A. A. Karyakin, O. V. Gitelmacher and E. E. Karyakina, *Anal. Lett.*, 1994, **27**, 2861–2869.
16 A. A. Karyakin, E. E. Karyakina and L. Gorton, *J. Electroanal. Chem.*, 1998, **456**, 97–104.
17 A. A. Karyakin, *Electroanalysis*, 2001, **13**, 813–819.
18 A. A. Karyakin and E. E. Karyakina, *Sens. Actuators, B*, 1999, **B57**, 268–273.
19 A. A. Karyakin, E. E. Karyakina and L. Gorton, *Anal. Chem.*, 2000, **72**, 1720–1723.
20 A. A. Karyakin, E. A. Puganova, I. A. Budashov, I. N. Kurochkin, E. E. Karyakina, V. A. Levchenko, V. N. Matveyenko and S. D. Varfolomeyev, *Anal. Chem.*, 2004, **76**, 474–478.
21 A. A. Karyakin, E. A. Puganova, I. A. Bolshakov and E. E. Karyakina, *Angew. Chem., Int. Ed.*, 2007, **46**, 7678–7680.
22 A. A. Karyakin, E. E. Karyakina and L. Gorton, *Electrochem. Commun.*, 1999, **1**, 78–82.
23 I. L. Mattos, L. Gorton, T. Laurell, A. Malinauskas and A. A. Karyakin, *Talanta*, 2000, **52**, 791–799.
24 M. Florescu and C. M. Brett, *Anal. Lett.*, 2005, **37**, 871–886.
25 R. Pauliukaite, M. Florescu and C. M. Brett, *J. Solid State Electrochem.*, 2005, **9**, 354–362.
26 R. Garjonyte and A. Malinauskas, *Sens. Actuators, B*, 1999, **B56**, 93–97.
27 N. A. Sitnikova, M. A. Komkova, I. V. Khomyakova, E. E. Karyakina and A. A. Karyakin, *Anal. Chem.*, 2014, **86**, 4131–4134.
28 J. J. GarciaJareno, J. NavarroLaboulais and F. Vicente, *Electrochim. Acta*, 1996, **41**, 2675–2682.
29 L. V. Lukachova, E. A. Kotel'nikova, D. D'Ottavi, E. A. Shkerin, E. E. Karyakinia, D. Moscone, G. Palleschi, A. Curulli and A. A. Karyakin, *IEEE Sens. J.*, 2003, **3**, 326–332.
30 N. A. Sitnikova, A. V. Borisova, M. A. Komkova and A. A. Karyakin, *Anal. Chem.*, 2011, **83**, 2359–2363.
31 N. A. Sitnikova, A. V. Mokrushina and A. A. Karyakin, *Electrochim. Acta*, 2014, **122**, 173–179.
32 S. Bharathi and O. Lev, *Appl. Biochem. Biotechnol.*, 2000, **89**, 209–216.
33 Y. Z. Guo, A. R. Guadalupe, O. Resto, L. F. Fonseca and S. Z. Weisz, *Chem. Mater.*, 1999, **11**, 135–140.
34 A. Salimi and K. Abdi, *Talanta*, 2004, **63**, 475–483.
35 A. V. Borisova, E. E. Karyakina, S. Cosnier and A. A. Karyakin, *Electroanalysis*, 2009, **21**, 409–414.
36 R. Koncki and O. S. Wolfbeis, *Anal. Chem.*, 1998, **70**, 2544–2550.
37 K. G. Stern, *Ber. Dtsch. Chem. Ges.*, 1933, **66**, 547–554.